Scaling of interfaces in brittle fracture and perfect plasticity

Eira T. Seppälä, Vilho I. Räisänen, and Mikko J. Alava
Laboratory of Physics, Helsinki University of Technology, P.O. Box 1100, FIN-02015 HUT, Finland
(Received 23 December 1999; revised manuscript received 16 February 2000)

The roughness properties of two-dimensional fracture surfaces as created by the slow failure of random fuse networks are considered and compared to yield surfaces of perfect plasticity with similar disorder. By studying systems up to a linear size $L=350$ it is found that in the cases studied the fracture surfaces exhibit self-affine scaling with a roughness exponent close to 2/3, which is asymptotically exactly true for plasticity though finite-size effects are evident for both. The overlap of yield or minimum energy and fracture surfaces with exactly the same disorder configuration is shown to be a decreasing function of the system size and to be of a rather large magnitude for all cases studied. The typical ''overlap cluster'' length between pairs of such interfaces converges to a constant with increasing L.

PACS number(s): 62.20.Mk, 62.20.Fe, 05.40.−a, 81.40.Np

I. INTRODUCTION

Roughness of fracture surfaces (FS's) is a currently topical problem that has opened up surprising connections between engineering and poorly understood questions of statistical physics. The simple questions of why and how a crack surface becomes rough has no easy answers since there is a multitude of experimental facts and ways for cracks to develop or propagate. One simplification, adopted in this work, is to neglect cases in which the prevalent feature is the propagation of ''fast'' cracks in favor of slow, adiabatic crack formation. The questions we address here are related to how disorder affects crack surfaces and how interfaces created by different load-elongation responses are related. Disorder is present in materials at all length scales in the form of atomic impurities, dislocations, grain boundaries, and so forth.

No generally accepted picture exists yet of how slow cracks are formed and how this process relates to crack interfaces [1]. In three dimensions there are indications that the cracks become self-affine above a certain intermediate length scale so that the roughness exponent ζ is close to 0.8. Moreover, the physics of crack advancement indicates that the generic features of phase transitions of driven lines (crack fronts in three dimensions) become relevant [2]. Quantitative agreement is missing, however. For slow fracture in two dimensions (2D) and at small length scales in 3D the interface scaling may be different in that the exponents are close to those of the minimum energy (ME) interface. These are the same as for the random exchange Ising model (REIM) domain walls at zero temperature, and have therefore the exact value $\zeta=2/3$ in 2D [3] and the approximate value 0.41 ± 0.01 in 3D [4–6]. The physics involved is simple: the crack minimizes up to the pertinent length scale the surface energy E given by

$$E=\int d^{d-1}\mathbf{x}[\Gamma\{\nabla z(\mathbf{x})\}^2+V_r\{\mathbf{x},z(\mathbf{x})\}], \qquad (1)$$

where the integral includes two contributions. One arises from a surface stiffness (proportional to Γ) due to the deviations $\nabla z(\mathbf{x})$ from a straight crack, and the second from a random disorder potential with a two-point correlator $\langle V_r(\mathbf{x}',z')V_r(\mathbf{x},z)\rangle$ where the disorder average is implied and $(\mathbf{x}',z')$, $(\mathbf{x},z)$ denote two locations inside the medium. The exponents quoted above are true when the disorder has pointlike correlations. The fluctuations of the potential would in an experiment correspond to a varying failure threshold or elastic modulus, etc., depending on the circumstances. The closeness of the numerical values of the roughness exponents gives rise to the intriguing question as to why a slow fracture should resemble a global optimization like ground state domain walls. The connection is suggested by the fact that, in arbitrary dimensions, lattice models that describe scalar perfect plasticity can be exactly mapped to REIM domain wall problems. For brittle fracture or vectorial failure problems in general, the correspondence is not obvious. Two-dimensional failure is special in that there is some experimental evidence of the crack roughness scaling with the domain wall in the REIM, i.e., the so-called directed polymer (DP) global roughness exponent [7]. This connection between global optimization and fracture surfaces has also been made in 2D simulations of brittle failure [8,9]. In 3D, it is still unclear whether even just the numerical models show such a universality [9–11].

In this paper we investigate in two dimensions the scaling properties of slow fracture surfaces and compare them to minimum energy surfaces with similar *a priori* disorder. We perform numerical simulations of the random fuse network (RFN) model, which has been studied extensively as a model of brittle failure of disordered materials [12–14]. As an introduction, we consider extensive system properties such as fracture stress, fracture strain, and damage. For the main case studied here, dilution-type disorder, these are found to be in good agreement with the critical-defect-type arguments proposed by Duxbury and co-workers [13] which imply logarithmic scaling with system size. Note that when compared with ''reality'' this kind of model contains two assumptions: first, the stress relaxation is supposed to be much faster than the stress rate (an adiabatic failure); and second, one assumes

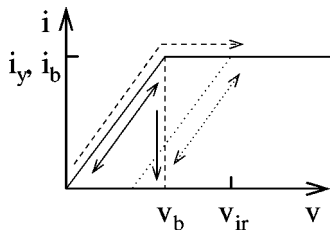

FIG. 1. The voltage-current diagram of a fuse or a medium. The $\leftrightarrow$ arrow describes ideal elastic behavior. The dashed line describes an ideal elastic breakdown at the critical current i_b with the corresponding voltage v_b. The dashed arrow describes perfect plasticity with yield current i_y, and the dotted arrow describes elastic-plastic behavior with an irreversible yield strain $v_{ir}-v_b$ at v_{ir}. The current as a function of voltage with the corresponding elastic or plastic behavior of the medium may increase or decrease only in the directions noted by the arrows.

that the energy released by local crack formation is dissipated with no effect on the crack propagation.

The paper starts with a short description of the numerical methods used and the dynamics of adiabatic crack formation in Sec. II. Section III discusses the strength properties of random fuse networks as a function of system size L. There are a number of ways to characterize a self-affine interface *a posteriori*. This is the main theme of Sec. IV, the topic of showing that 2D brittle fracture interfaces have DP-type scaling. We demonstrate how both the so-called local width and the statistical properties of ensembles of interfaces indicate a similar kind of self-affine scaling. The scaling exponent is seen to be close to the DP one, $\zeta=2/3$. The section also contains numerical data for varying disorder strength, and in particular compares perfect plasticity and brittle fracture by measuring the overlap of the associated interfaces starting with the same disorder configurations. This would be particularly relevant should it be that the fracture and yield interfaces use the same ''valley'' in the landscape of the energies or thresholds. The paper finishes with a discussion in Sec. V.

II. CREATING THE INTERFACES

A. Numerical models

Random fuse networks are electrical analogs of elasticity and failure with disorder incorporated. One usually sets out to mimic a tensile test, implying that the extensive thermodynamic parameters become V_{ext} and I_{ext}, external voltage and current, respectively. These correspond to displacement and force in a real experiment. To study brittle failure one defines the elements that connect two nodes on an original lattice as *fuses*. These have a linear voltage-current relationship until a breakdown current i_b; see Fig. 1. A second choice would correspond to perfect plasticity, if one made the fuses such that the local current becomes irreversibly constant at i_y and stays so unless the local voltage is reduced, in which case the conductivity becomes the original one and there is a permanent *yield strain*.

In the following we use two different numerical techniques to study both brittle and perfectly plastic RFN's. Brittle failure is studied with standard adiabatic fracture iterations. These consist of solving the current balance in the system from Kirchhoff's and Ohm's laws and breaking after each iteration the most strained fuse [the criterion is $\min(i_j/J_{c,j})$, where i_j is the local current in each of the fuses and $J_{c,j}$ is the local threshold]. The currents and voltages are found by solving the linear system of currents by the conjugate-gradient method.

For perfect plasticity we use a mapping to minimum energy interfaces, i.e., random exchange Ising domain walls in their ground state, where exchange constants J_{ij} between nearest neighboring spins are random but non-negative. In some cases we have exactly the same quenched disorder (equal thresholds for failure i_b and yielding $i_y\equiv 2J_{ij}$ for each fuse) as for brittle failure, and in the following the threshold for a fuse in both cases is denoted by J_c. The simulations are done using combinatorial optimization: finding the yield path (in 2D) is equivalent to the minimum cut-maximum flow problem of network flows [15] that minimizes $\Sigma_{interface} i_y$. This technique is more convenient than transfer matrix methods in that there are no restrictions for the shape of the optimal path as overhangs and arbitrary transverse steps are included in a natural fashion.

The typical choice for introducing disorder to a RFN is to pick the failure currents J_c from a prescribed probability distribution $P(J_c)$. The important issue is the behavior of P for $J_c\simeq 0$ and for $J_c\to\infty$; the tails of the distribution are known to have strong effects on the strength properties and damage accumulation in the case of brittle fracture. For perfect plasticity or directed polymers the case is much simpler in that for one-dimensional interfaces in $(1+1)$-dimensional systems such pointlike disorder is, in the renormalization group sense, always relevant. Thus one expects always the same scaling properties in terms of interface roughness and sample-to-sample interface energy fluctuations; these correspond to yield stress fluctuations in plasticity. The amplitudes, however, are nonuniversal and thus will depend on the exact form of P.

In the following we study as typical examples the cases where $P(J_c)$ is a flat distribution $[P(J_c)=1/(2\,\delta J)$ for $J_0-\delta J\leqslant J_c\leqslant J_0+\delta J]$ and where P corresponds to ''dilution disorder.'' That is, $P(J_c)=p\,\delta(J_c-1)+(1-p)\,\delta(J_c)$. The fraction of fuses that remain for infinitesimal currents with dilution is denoted by p, which has a value $p=0.8$ unless otherwise mentioned, as for the uniform distribution case $\delta J/J_0=1$. The systems are chosen so that the direction of macroscopic current flow is aligned in the $\langle 10\rangle$ orientation of the square lattice, having periodic boundaries in the perpendicular direction. The systems are isomorphic, i.e., $L_x=L_z$, and their sizes range from $L^2=10^2$ to 350^2 for brittle failure and to 1000^2 for perfect plasticity. The mean positions of the surfaces are not fixed; hence they may be anywhere in the system. The interfaces are defined in the usual way so that, in the case of overhangs, the so-called solid-on-solid approximation is used, i.e., the interface is found by taking the furthest value of the interface with respect to a fixed end of the network. The number of realizations N over which the disorder averaging is performed is limited by the CPU time for simulations of brittle fracture. In the case of plasticity, the technique used leads to a roughly linear scaling with respect to the number of fuses in a system, regardless of the threshold distribution. The number of different random realizations is shown in Table I for the cases in which exactly the same

TABLE I. The number of realizations N performed in simulations for exactly the same randomness of brittle failure and plasticity.

	Dilution, p		Uniform, $\delta J/J_0$	
L	0.8	0.85–0.97	1	0.1–0.8
10, 20	760			
30–90	760		66	
100	370	537	248	250
200	370			
275, 350	250			

random networks are studied for both brittle failure and perfect plasticity. If only the ME surfaces are studied $N = 200–5000$.

B. Formation of the interfaces

One should note that if fracture surfaces have nontrivial geometric scaling properties and in particular resemble directed polymers (in 2D) this opens up several further questions: whether the outcome is independent of disorder strength, whether the disorder is always relevant as for 2D minimum energy surfaces, and how the surface roughness relates to other typical quantities. The standard way of iterating fracture in fuse networks, whether perfectly plastic or brittle, is based on extremal dynamics. The condition $\min(i_j/J_{c,j})$ for the failure of the next element contains two effects: the disorder through the threshold and the local current, which depends on the environment of the fuse.

For perfect plasticity, the information necessary for finding the final yield surface is contained in the initial field $J_{c,j}$ due to the monotonicity property noticed by Roux and Hansen [16]. Even if one simulates the development of the system as a series of fuse network problems (the tangent problem), the local current never decreases in a yielding process. Thus the final yield surface equals a blocking configuration that can be calculated from the original thresholds. This is related to the fact that the surface is made much faster to compute than the whole process by considering it as an optimization problem for the interface: the history of the whole process or system involves much more information.

For brittle fracture the monotonicity property is not true and thus no direct mapping exists between the initial disorder and a quantity to be minimized. The mapping of perfect plasticity to fuse networks makes it clear, on the other hand, that the difference between the processes is smaller than it would seem at first glance. This is because in the tangent algorithm one has to solve a series of adiabatic failure problems with the local yield thresholds i_y renormalized by subtracting the current already passing through the fuse. Nonetheless, each failure iteration is affected by stress-enhancement effects exactly as in a failure problem with the same fuses still intact. For brittle failure, the implication of the stress enhancements during the failure process is that in order to obtain a minimum energy surface [as defined by Eq. (1)] the original disorder $i_{b,j}$ has to be *renormalized*. That is, the thresholds or missing fuses contain frozen-in information about how the field of local stresses will develop and normalize the local thresholds $i_{b,j}$ in the failure criterion. Considered in this light, it is sensible to consider brittle fracture surfaces as ''blocking paths,'' too. Yet the question remains whether the interfaces are still in the same *universality class*: if the correlations in the renormalized disorder become different enough from pointlike correlations the interface scaling properties will change. For example, columnar correlations [$V_r(\mathbf{x},z)$ constant along x_i or z] would be relevant in this respect.

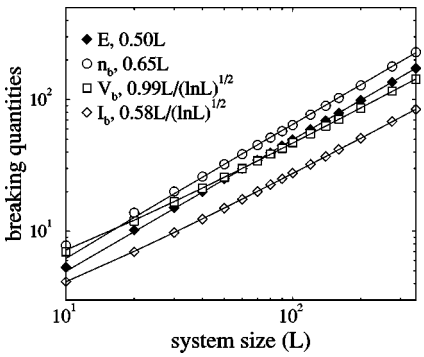

FIG. 2. Scaling of energy of ME surfaces, closed diamonds, and fracture quantities: total damage, i.e., number of broken fuses n_b, open circles; breaking voltage V_b of the network, open squares; and breaking current I_b of the network, open diamonds, as a function of the system size L. The disorder is dilution type with $p=0.8$. The number of realizations N for the brittle failure case is shown in Table I. For ME surfaces $N=5000$ for $L^2=10^2–50^2$, $N=1000$ for $L^2=60^2–350^2$. The lines are least-squares fits, linear for E and n_b, $L/\sqrt{\ln L}$ for V_b and I_b, to the data.

III. SCALING OF FRACTURE

A fracture can be contrasted with perfect plasticity also by looking at extensive thermodynamic quantities. The standard ones to consider are the damage n_b, the number of fuses broken in total, and the failure current I_b and voltage V_b as computed from the maximum current of the IV curve. For ''truly'' brittle failure this definition of V_b agrees with that defined as the end point of the IV curve. In the failure of brittle fuse networks there is considerable evidence for the relevance of critical-defect-type effects. That is, the defect with the largest current enhancement will dictate the scaling of the current and voltage. For yield surfaces one would have $I_y=E\sim L$, $\Delta E\sim L^\theta$ where $\theta=2\zeta-1$ and ζ is the roughness exponent. Thus the critical strength quantities, without the renormalization discussed above, are supposed to have different scaling behavior in plasticity and fracture.

Figure 2 shows the scaling of damage and the strength quantities for dilution-type disorder, $p=0.8$. The lines in the figure have been found with least-squares fits to data using the assumptions of linear scaling for n_b and for the other two quantities the scaling $V_b, I_b \sim L/\sqrt{\ln L}$, which comes from the extreme value statistics, i.e., the Gumbel distribution, studied in the fracture case by Duxbury and coauthors [13]. It is seen that the scaling of the number of broken fuses is asymptotically very close to a linear one. This means that the system still breaks in a brittle mode for $p=0.8$. For V_b and I_b the scaling in the whole regime beautifully follows the $L/\sqrt{\ln L}$ scaling. Notice that the surface energy of yield surfaces is in principle a lower limit for n_b and that both scale linearly.

One sees that the energy of yield surfaces or the lower limit for n_b is lower by a constant factor than n_b of fracture surfaces. Similar behavior is visible in the roughness values of the fracture and yield surfaces studied in the next section.

IV. SCALING OF INTERFACES

A. Global and local interface width

There are several ways to characterize the scaling properties of interfaces. Consider the case where an interface is defined as a function of $\mathbf{x}$ as $z(\mathbf{x})$. The standard way of looking at scaling properties is to calculate the interface width [17] or standard deviation, i.e., the so-called root-mean-square roughness,

$$w=\left\langle \frac{1}{L^{d-1}}\sum_{x=1}^{L^{d-1}}[z(\mathbf{x})-\overline{z}]^2\right\rangle^{1/2}, \tag{2}$$

where $\overline{z}$ denotes the mean position of an interface and $\langle\rangle$ the disorder average over the different random configurations. If the interface is self-affine, w should scale with L^{ζ}, ζ being the roughness scaling exponent. For self-affine interfaces the scaling exponent ζ is expected to be valid also for higher-order statistics. This is seen for the height-height correlation functions $G_k(l)=\langle|z(\mathbf{x})z(\mathbf{x}+l)|^k\rangle$ and is applicable to the local width as well. Note that there is no *a priori* reason to use a Family-Vicsek-type of scaling ansatz with a correlation length [18], since there is no dynamical length scale for these interfaces. This is an assumption for brittle failure, and it will be shown to hold by our data below, and is moreover exactly true for perfect plasticity. It is also theoretically appealing since slow, adiabatic failure does not involve any time scale.

The local width in two dimensions is defined analogously to the global interface roughness w with

$$w_{loc}^2(l)=\left\langle \frac{1}{l}\sum_{x=1}^{l}[z(x)-\overline{z_l}]^2\right\rangle, \tag{3}$$

where the local interface height $\overline{z_l}$ is averaged over windows of size $l\leqslant L$. One should note the obvious connection to G_2 that exists for both the local and global definitions of interface width.

The advantage of using more complicated indicators of scaling is that one can draw conclusions based on data in a much more limited system size range than with the global interface width. Of course, such *a posteriori* techniques are most commonly used in the context of characterizing experimental fracture surfaces. Here we note the fact that for small L finite size effects make it rather difficult to determine the roughness exponent (if one assumes the interfaces to be truly self-affine to begin with). This is especially true for 3D systems for which the computational costs easily become prohibitive.

The global interface roughness w as a function of system size is compared between directed polymers and brittle fracture interfaces with dilution-type disorder and uniform distribution of J_c in Fig. 3. As expected, for small L the systems suffer from finite size effects, having exponent greater than $\zeta=2/3$, but eventually the exponent becomes comparable to the value one obtains by fitting a power law to the large-L data. Specifically, in the dilution case, Fig. 3(a), the effective exponent for the fracture surfaces is $\zeta_{\mathrm{FS}}\simeq 0.82$ and for the minimum energy interfaces with exactly the same random threshold configurations $\zeta_{\mathrm{ME},<}\simeq 0.74$. For larger system sizes, which we are able to study numerically only in the plasticity limit with large enough number of realizations, $\zeta_{\mathrm{ME},>}\simeq 0.67$. For the fuses from the uniform random distribution, Fig. 3(b), the fracture surfaces scale with $\zeta_{\mathrm{FS}}\simeq 0.73$ and the yield surfaces from the networks with exactly the same random configurations have $\zeta_{\mathrm{ME},<}\simeq 0.74$. Hence the finite sizes effects seem to be more similar between the processes than in the dilution case. For larger system sizes of minimum energy interfaces $\zeta_{\mathrm{ME},>}\simeq 0.69$.

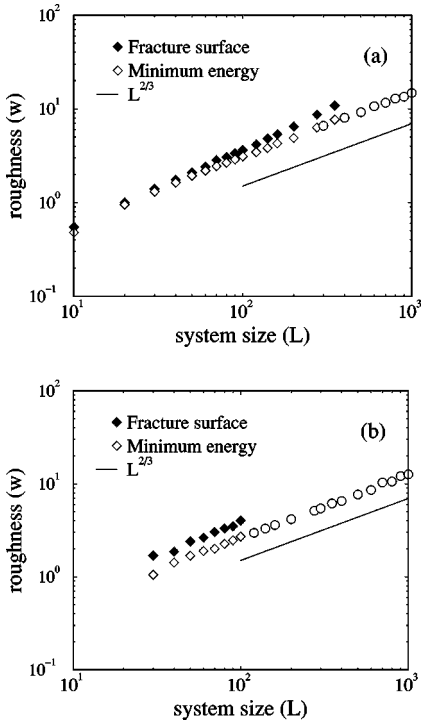

FIG. 3. The interface width w versus the system size L for brittle fracture interfaces, closed diamonds, and the minimum energy ones, open diamonds, from the same random networks. Open circles are minimum energy interfaces from larger system sizes. The disorder is (a) dilution type with $p=0.8$ and (b) from uniform distribution of fuse thresholds with $\delta J/J_0=1$. The number of different random realizations for exactly the same fracture and yield surfaces is shown in Table I. ME surfaces have $N=1000$ for $L^2=300^2,400^2$, $N=500$ for $L^2=500^2-700^2$, and $N=200$ for $L^2=800^2-1000^2$ in (a), $N=500$ for $L^2=120^2-400^2$ and $N=200$ for $L^2=500^2-1000^2$ in (b). The lines are guides to the eye with a slope $\zeta=2/3$.

Figure 4 compares the local width of directed polymers to the brittle fracture interface for dilution-type disorder with $p=0.8$. For directed polymers one sees that the $\zeta=2/3$ scaling is valid for larger system sizes in the region where the window size $l\leqslant\frac{1}{5}L$. With open boundary conditions the scaling region would be larger. However, for smaller system size $L^2=100^2$ there is a visible amplitude difference compared to the larger system sizes. The fracture surfaces show similar behavior but have larger finite size effects when compared to the yield surfaces, and they have a larger amplitude, too, than minimum energy surfaces in local and in global width scaling.

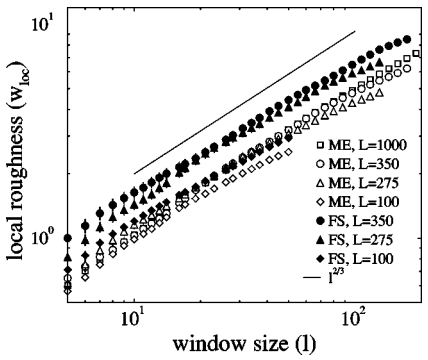

FIG. 4. The local interface roughness w_{loc} versus the window size l for the dilution type of disorder with $p=0.8$. The system size $L^2=1000^2$ has $N=2000$, while for all the other system sizes the data are from the same configurations as the data in Fig. 3(a). The line is a guide to the eye with a slope $\zeta=2/3$. For the minimum energy interfaces the $\zeta=2/3$ scaling is seen in a region $l<(1/5)L$ for larger system sizes, while $L^2=100^2$ has a visible amplitude difference. Periodic boundaries are used in the transverse direction of the external voltage. The correlation between the local width of the elastic fracture and plastic yield surfaces is clearly seen.

Our result supports the conclusion of Ref. [9] that 2D brittle fracture surfaces are in the directed polymer universality class ($\zeta=2/3$), although due to the stronger finite size effects the asymptotic region is harder to reach than for yield surfaces.

B. Roughness statistics

Next we address the higher-order statistics of fracture surfaces. For directed polymers one knows that the end-point transverse deviation distribution $z(x)$ [$x(t)$ in the ordinary DP notation], is roughly Gaussian for the standard case of one fixed and one free end (see, e.g., [3]) and follows a scaling form $P[z(L)]\sim f(z/L^{\zeta})$. One can likewise write down a scaling form for the interface energy. Next we assume that the brittle fracture interfaces obey similar self-affine scaling and study the roughness probability distribution $P(w,L)$ as a function of L (we concentrate on the $p=0.8$ case of the previous subsection). Figure 5 shows a typical example of such a distribution: it is not centered around zero and is reminiscent of a log-normal or Poissonian distribution. This can be understood qualitatively since the roughness w is also a measure of the nonzero maximum transverse displacement z. The figure includes a distribution for ME surfaces from the same systems, too.

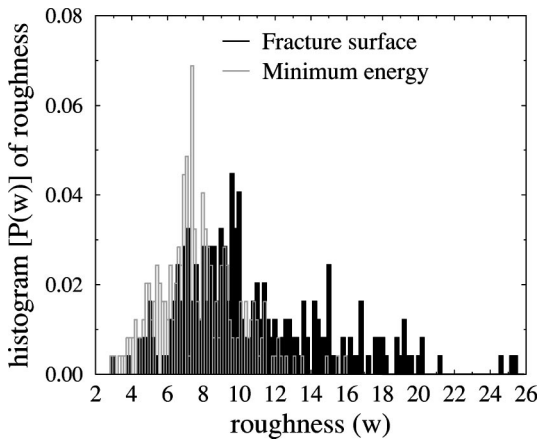

FIG. 5. The histogram $P(w)$ of the roughness for the ideal elastic and perfect plastic yield surfaces in systems of size $L^2=350^2$ and dilution type of disorder with $p=0.8$. The data are from the same configurations as the data in Fig. 3(a).

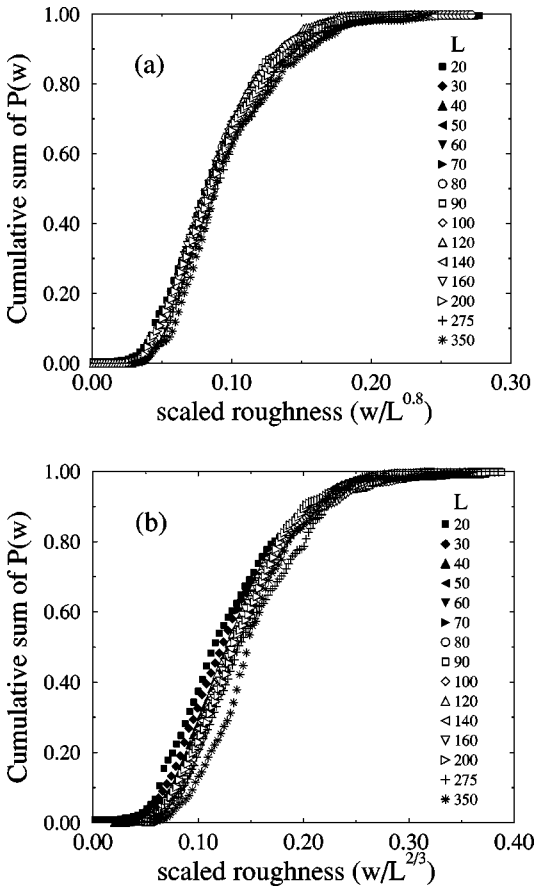

FIG. 6. Cumulative sums of $P(w)$ for both fracture (a) and minimum energy surfaces (b) for various system sizes with dilution type of disorder, $p=0.8$. The data are from the same configurations as the data in Fig. 3(a). The data have been scaled with $L^{0.8}$ in (a) and with $L^{2/3}$ in (b).

As one could see already in the previous subsection, the 2D fracture surfaces are rougher than the minimum energy surfaces (i.e., assuming self-affine scaling in both cases, the amplitude of the roughness w/L^{ζ} is larger for FS's). This is visible here also, since the distribution of $P(w)$ is not only wider but extends to higher values for the fracture case. While assuming that $P(w)$ follows the same self-affine scaling law as $P[z(L)]$ we may study the disorder standard deviation

$$\sigma(w)=\langle(w-\overline{w})^2\rangle^{1/2}, \tag{4}$$

where w is from a single random system and $\overline{w}$ is the global disorder-averaged roughness calculated using Eq. (2). $\sigma(w)$ scales with $L^{2/3}$, too, although the data are more scattered due to the fact that higher-order statistics are always more vulnerable to the finiteness of the statistics than the integral of them.

In Fig. 6 we collapse the data of the cumulative sums of the distributions $P(w,L)$ for various L. For both kinds of

interface the data collapse is better with exponents $\zeta > 2/3$, which is due to the finite size effects. For fracture surfaces $\zeta = 0.8$, as in Fig. 3(a), seems to work nicely, and for the yield surfaces $\zeta = 0.74$ would be better than $\zeta = 2/3$. In our opinion the figure justifies the assumption of an asymptotically self-similar scaling of $P[w(L)] \sim f(w/L^{\zeta})$.

C. Scaling of overlap quantities

The average overlap P_O of fracture and minimum energy surfaces as a function of the system size for the dilution case is seen in Fig. 7(a). Overlap is defined as the fraction of the disorder realizations in which at least one (x,z) coordinate pair is common between the fracture and yield surfaces. Clearly the overlap is reduced as a function of the system size. This is not surprising, because with increasing system size the probability of the first breaks taking place at the globally weakest place decreases. However, if one expects the overlap quantity to originate from the result of depositing the surfaces randomly (like particles of finite width on a 1D line segment of length L), one obtains $P_{ran} = (A_{\mathrm{FS}} w_{\mathrm{FS}} + A_{\mathrm{ME}} w_{\mathrm{ME}})/L$. A_{FS} and A_{ME} are prefactors needed to compute the typical geometrical extent from the roughness values w_{FS} and w_{ME}. In the figure we have plotted P_{ran} from the same RFN configurations as P_O, with $A_{\mathrm{FS}} = A_{\mathrm{ME}} = 7.5$, which is a rather large value to be realistic; hence $P_O \not\equiv P_{ran}$. In the figure P_{ran} has a slope $\simeq -0.2$ while the asymptotic scaling according to the random deposition argument should be $P_{ran} \sim L^{-1/3}$. For small systems the average overlap is very large, of the order of 0.5 in the particular case studied here.

Figure 7(b) shows the average size $\langle s \rangle$ of overlapping clusters. The overlapping cluster is defined as the number of neighboring common (x,z) coordinate pairs. The overlap cluster size saturates at $\langle s \rangle \simeq 8.5$. Figure 7(c) shows the average total length of the overlap in configurations that do have an overlap, i.e., $(\Sigma s)/N_O$, where $N_O = P_O N$. One may write $(\Sigma s)/N_O = (\langle s \rangle N_s N_O)/N_O = \langle s \rangle N_s$, where N_s is the number of overlap clusters in a system that has overlaps. By assuming that $N_s \sim L$ and $\langle s \rangle = \mathrm{const}$, we get $(\Sigma s)/N_O \sim L$, which is demonstrated in the figure. Since in the large-L limit $(\Sigma s)/N_O = C_1 L + C_2$, $C_2 \simeq 23$, there is a crossover in systems of size $L \simeq 27$, because in the small-system-size limit Σs must be smaller than L. On the other hand, $C_1 = 0.15$ tells us that approximately 15% of the length of the fracture and yield surfaces are overlapping with each other. The scenario is that if the fracture happens to start from the same minimum energy valley where the DP is located, it will naturally stay localized there; however, the associated surface stiffness is weaker and thus the excursions. Notice the saturation of the cluster size, which agrees with the scenario.

Figure 8 shows four examples of what happens with varying disorder strength $\delta J/J_0$ for $L = 100$. The subplots demonstrate several effects. For the weakest disorder, both the interfaces are nevertheless ''rough'' (i.e., not flat), which shows that in spite of a single, growing crack even the brittle fracture case can produce a crack that fluctuates in the transverse direction. The qualitative behavior is the same for both cases; note that for the yield surfaces one expects a Larkin length scale on which the interfaces look flat due to the competition between disorder and elasticity. With increasing disorder the crack is finally localized in the lower part of the system—the threshold field is rescaled in all the cases with the ''initial'' random number being kept constant. Meanwhile, the damage for brittle fracture grows strongly. Notice

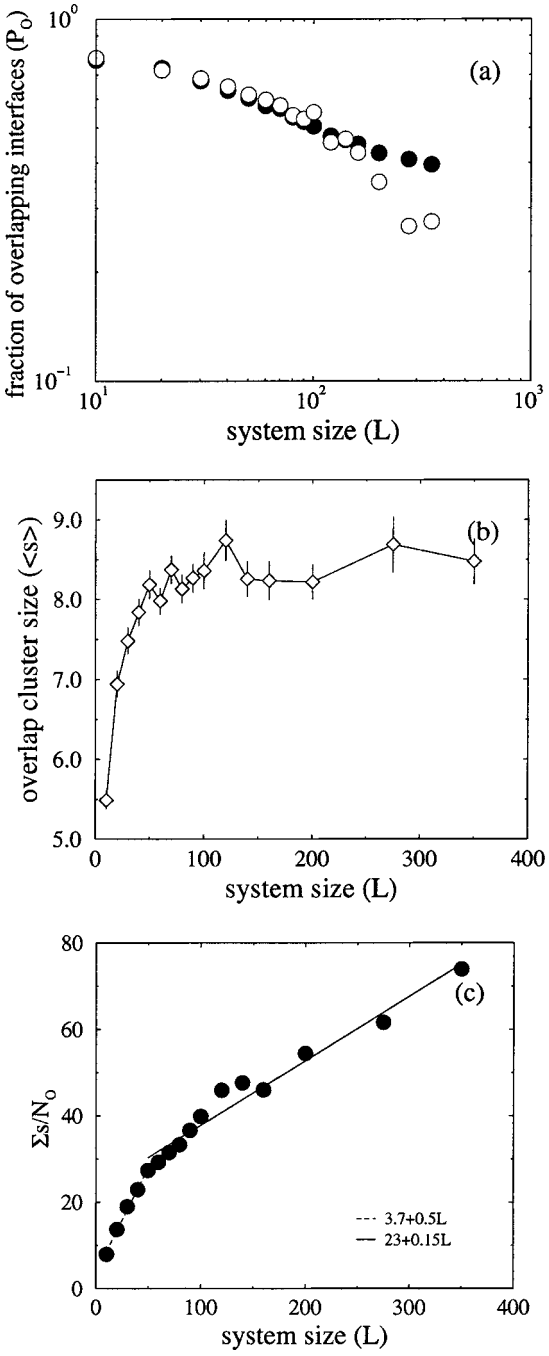

FIG. 7. (a) Fraction of the disorder configurations, P_O, in which the fracture surface and the minimum energy interface do have an overlap, i.e., at least one common (x,z)-coordinate pair, open circles. The disorder is dilution type with $p = 0.8$. The data are from the same configurations as the data in Fig. 3(a). The closed circles are for comparison with the value $P_{ran} = 7.5(w_{\mathrm{FS}} + w_{\mathrm{ME}})/L$ from Fig. 3(a); see the text for details. (b) The average size $\langle s \rangle$, i.e., the number of common neighboring (x,z)-coordinate pairs, of the overlapping clusters as a function of the system size. The overlap cluster size saturates at $\langle s \rangle \simeq 8.5$. (c) The total length of overlap in configurations that do have an overlap in their interfaces, $\Sigma s/N_O$. The lines are linear least-squares fits to the data.

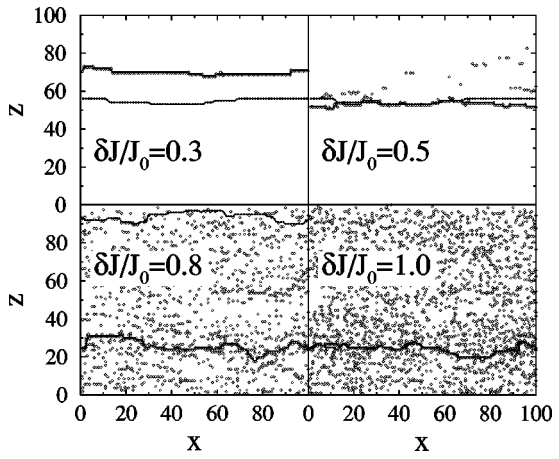

FIG. 8. Examples of final damage (diamonds) and the respective brittle failure (solid line) and yield (dotted line) surfaces for $\delta J/J_0=0.3$, 0.5, 0.8, and 1.0. The system sizes are $L^2=100^2$, and the random initial configuration in each system is the same, but the J_c's are rescaled with the corresponding δJ. For $\delta J/J_0=1$ the total overlap of fracture and yield surfaces $\Sigma s=85$.

how the yield (minimum energy) surface moves in the system as $\delta J/J_0$ is changed. For the two cases with weakest disorder the surface stays the same. In two of the subplots there is considerable overlap between the fracture and the yield surfaces: $\delta J/J_0=1$ leads to a total overlap of $\Sigma s=82$.

Figure 9 shows the dependencies of the roughness and overlap quantities on the disorder strength. Both for the dilution case, Fig. 9(a), and for systems with randomness from the uniform distribution, Fig. 9(b), the fracture and yield surfaces are always rough, except for the finite size effects in the small-$\delta J/J_0$ limit. Even in this case the strong disorder fixed point is attractive and we simply have the result that the system size is smaller than the Larkin length above which the asymptotic behavior is seen. The roughness increases with decreasing p until the bond-percolation limit $p_c=1/2$ is reached and the surfaces become fractals, with the corresponding hull exponent. In the insets the average overlap P_O and the average overlapping cluster size $\langle s\rangle$ are shown. P_O increases for both types of disorder with increasing disorder strength, except in the infinitesimal disorder, $p=1-\epsilon$ and $\delta J/J_0=\epsilon$, limits, where it naturally diverges; the same is true for $\langle s\rangle$ even with finite disorder. In order to compare P_O with the random deposition argument, P_{ran} is plotted from the data of the same configurations with $A_{\mathrm{FS}}=A_{\mathrm{ME}}=8$ showing again $P_O\neq P_{ran}$. $\langle s\rangle$ seems to saturate with increasing disorder strength for both types of disorder around $\langle s\rangle \simeq 8-10$, which might be a coincidence, since one could guess it to be disorder-type dependent.

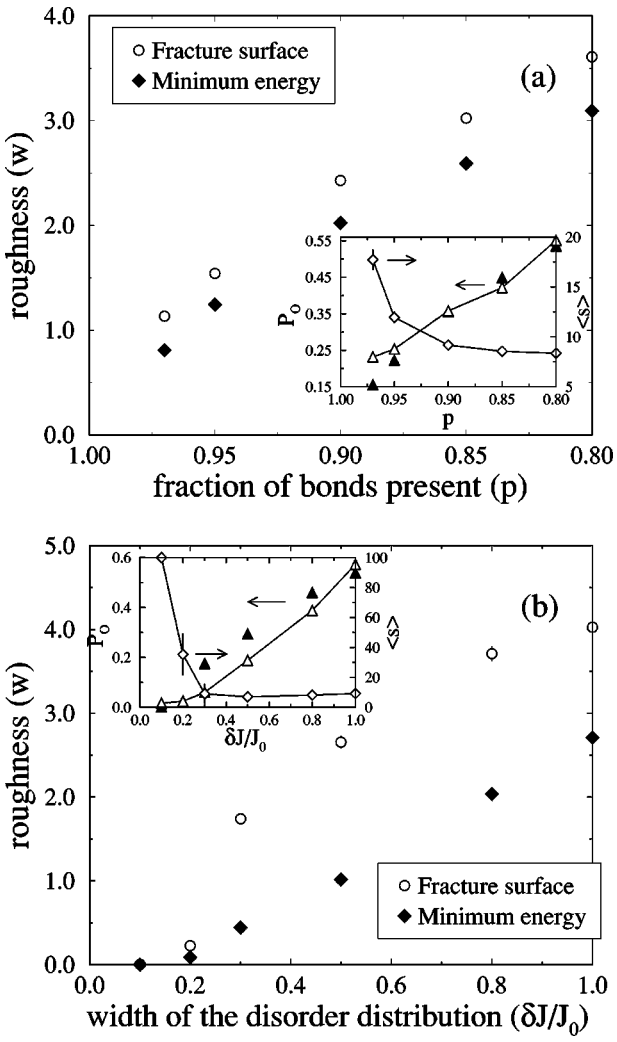

FIG. 9. Interface width w of the fracture and minimum energy surfaces with varying disorder strength for the dilution type of disorder (a) and uniform distribution of fuse thresholds (b). The system size $L^2=100^2$ for each system and the number of realizations is shown in Table I. The insets show for the same systems the fraction of overlapping disorder configurations P_O, open triangles, P_{ran} with $A_{\mathrm{FS}}=A_{\mathrm{ME}}=8$ in both cases, closed triangles, and the average overlapping cluster sizes $\langle s\rangle$, diamonds, as a function of the disorder strength.

V. DISCUSSION

This paper has explored the connections between brittle fracture and minimum energy surfaces. We have given numerical support for the idea of these being in the same universality class in two spatial dimensions. This argument is based on the scaling of interface width and local roughness and the statistics of ensembles of interfaces. For both scalar brittle fracture and perfect plasticity, or minimum energy, interfaces these turn out to have similar scaling properties, indicating that brittle fracture interfaces have a roughness exponent of 2/3 (as for directed polymers) and are also truly self-affine. In spite of the fact that we have studied only two types of disorder distribution, we nevertheless believe that the numerics points to a picture of asymptotically rough cracks in spite of the stress-enhancement effects, which one would expect to play a role in brittle fracture with a large, dominating crack. Such is the case in particular for dilution-type, relatively weak disorder, a main part of our study. Notice that for weak disorder even minimum energy surfaces tend to be relatively flat as the amplitude of the roughness is small.

The results presented earlier were obtained for systems that were governed by extreme scaling-type arguments. The role of the disorder can be tested in another way, more relevant to standard fracture surface experiments, by introducing a notch, or a row of prefailed fuses. The current distri-

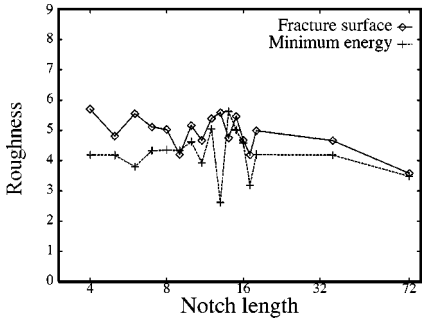

FIG. 10. Roughness of fracture and minimum energy surfaces in a notched sample with varying notch length. The system sizes are $L^2=100^2$ and the disorder is dilution type with $p=0.8$.

bution around the crack tip is a combination of the enhancement effect of the crack plus the additional fluctuations created by possible off-path or fracture process zone damage. Born-model simulations by Caldarelli *et al.* [19] show that self-affine cracks can avoid surface tension effects, i.e., they do not straighten out, if started from point seeds. In our case the question becomes whether the effective surface tension of the notch plus the grown crack wins over disorder, remembering that the stress enhancement for a symmetric crack is largest on axis. This is a necessary mechanism for any self-affine behavior, whether of the minimum energy surface universality class or not. Figure 10 shows the interface roughness of yield and brittle fracture surfaces for a fixed system size and varying notch length. It transpires that for both ME and brittle fracture surfaces the notch effect does not imply the flattening. Note the earlier arguments that yield surfaces have a *higher* surface tension. This is again due to the memory effect, which renormalizes the thresholds in the tangent problems so that they are smallest on the crack axis.

There are several experimental indications of the conclusion that brittle fracture interfaces exhibit self-affine behavior, with a roughness exponent close if not equal to the perfect plasticity one. Experiments done on real materials can bridge the gap between the two extreme limits. For such studies the expected behavior would in 2D, assuming slow failure, be self-affine as well. The extraction of the roughness exponent has been done here using the local width as a measure. For ensembles of experiments one should note the statistical implications of the scaling of the roughness distribution width and of the shape of the width probability distribution. The relative ''irrelevance'' of a notch hints about the possibility of pinning-center-like scaling properties, as should be true for the perfect plasticity case: the notch pins the final crack with certainty if it is large enough.

Finally, we note that there is no rigorous theoretical argument that would explain why brittle fracture seems to follow ME-type scaling. Indeed, we have here studied only the scaling of the interface roughness, and the aspect of interface energetics in terms of, e.g., the energy fluctuation exponent θ has been left aside. Notice that the bare strength properties are governed by logarithmic effects in the case of brittle failure. For brittle fracture interfaces to result from global optimization the initial failure thresholds have to be renormalized by the correlations that the stress intensities of the crack history induce. For such extremal statistics processes no theory exists for the time being, unlike the case of the quenched Laplacian breakdown model for which one can use real-space renormalization [20].

ACKNOWLEDGMENTS

The authors would like to thank the Finnish Cultural Foundation (V.R.) and the Academy of Finland for financial support through the Matra program.

[1] E. Bouchaud, J. Phys.: Condens. Matter **9**, 4319 (1997).
[2] P. Daguier, B. Nghiem, E. Bouchaud, and F. Creuzet, Phys. Rev. Lett. **78**, 1062 (1997).
[3] T. Halpin-Healy and Y.-C. Zhang, Phys. Rep. **254**, 215 (1995).
[4] D. Fisher, Phys. Rev. Lett. **56**, 1964 (1986).
[5] A. A. Middleton, Phys. Rev. E **52**, R3337 (1995).
[6] M. J. Alava and P. M. Duxbury, Phys. Rev. B **54**, 14 990 (1996).
[7] J. Kertész, V. K. Horvath, and F. Weber, Fractals **1**, 67 (1993).
[8] A. Hansen, E. L. Hinrichsen, and S. Roux, Phys. Rev. Lett. **66**, 2476 (1991).
[9] V. I. Räisänen, E. T. Seppälä, M. J. Alava, and P. M. Duxbury, Phys. Rev. Lett. **80**, 329 (1998).
[10] V. I. Räisänen, M. J. Alava, and R. M. Nieminen, Phys. Rev. B **58**, 14 288 (1998).
[11] G. G. Batrouni and A. Hansen, Phys. Rev. Lett. **80**, 325 (1998).
[12] *Statistical Models for the Fracture of Disordered Media*, edited by H. J. Herrmann and S. Roux (North-Holland, Amsterdam, 1990), Chaps. 4–7.
[13] P. M. Duxbury, P. L. Leath, and P. D. Beale, Phys. Rev. B **36**, 367 (1987); Phys. Rev. Lett. **57**, 1052 (1986).
[14] B. Kahng, G. G. Batrouni, S. Redner, L. de Arcangelis, and H. J. Herrmann, Phys. Rev. B **37**, 7625 (1988).
[15] M. Alava, P. Duxbury, C. Moukarzel, and H. Rieger, in *Phase Transitions and Critical Phenomena*, edited by C. Domb and J. L. Lebowitz (Academic Press, London, in press).
[16] S. Roux and A. Hansen, J. Phys. II **2**, 1007 (1992).
[17] Z. Rácz and M. Plischke, Phys. Rev. E **50**, 3530 (1994).
[18] Compare, e.g., A.-L. Barabási and H. E. Stanley, *Fractal Concepts in Surface Growth* (Cambridge University Press, Cambridge, U.K., 1995).
[19] G. Caldarelli, C. Castellano, and A. Vespignani, Phys. Rev. E **49**, 2673 (1994).
[20] R. Cafiero, A. Gabrielli, M. Marsili, L. Pietronero, and L. Torosantucci, Phys. Rev. Lett. **79**, 1503 (1997).